Field Map Error Location and Correction for Fat/Water Separation Methods

Purpose

To improve robustness of fat-water separation methods to swapping errors on 7T small animal scanners through image processing innovations that automatically detect and correct errors in the field map *ex post facto*.

Introduction

Quantification of fat by magnetic resonance imaging (MRI) can be used for monitoring fatty infiltration of the liver(1,2). In phase-based Dixon methods, chemical parameters are estimated by modeling the signal as a function of the phase differences caused by the chemical and field inhomogeneity shifts(3). As a result, the cost function is periodic with multiple minima per period(4,5). This ambiguity can lead to local "swaps" of fat and water, where the fat estimate appears in the water parameter map, and vice versa. The ambiguity cannot be resolved from the data itself, but its effect can be mitigated by including *a priori* knowledge of field smoothness in the estimation procedure. This done by formulating the cost function as the sum of the cost of assigning a particular guess to a pixel, and the cost of assigning a guess different from the neighboring pixels, and solving the resulting cost function with network algorithms such as Iterated Conditional Modes (ICM)(5,6). However, enforcing local smoothness does not necessarily ensure correct decomposition of fat and water at every pixel because of what we call "clumping errors", i.e., regions with sufficient cohesiveness to result in partial (part of the image) swaps and/or complete (the entire image) swaps. Swapping errors are a particular problem at 7T due to field inhomogeneity, which prevents automatic analysis of animal images for high throughput scanning of mouse models of disease.

Methods

12 animal volume data sets (total of 134 images) were acquired for various purposes unrelated to this study with IACUC approval using wild-type Bl/6 mice. The 2-D asymmetric RARE acquisitions were performed on a Bruker BioSpec 7T/30cm system, with echo delays(7) of 7.93e-5, 3.96e-4 and 7.14e-4 s. The analysis was performed in MATLAB (MathWorks, Inc., Natick, MA), on a 3.2GHz/8GB RAM computer (iBUYPOWER, Inc., Los Angeles, CA).

First, we ran FLAWLESS on each image volume. Then, we detected partial swap errors with a hole-filling algorithm that computed spatial gradients, which were much larger between unswapped and swapped regions than within each region. Discontinuous regions inside the animal were found by flood-filling a thresholded gradient map. We replaced the error regions with the median of the rest of the field map and used the result as an initial guess for a new run of ICM. Second, we developed a histogram analysis to correct partial swaps. Since the difference between correct and swapped regions is much larger than the spread within each region, the swaps were detected by segmenting the field map with k-means clustering. Each group that was significantly different from the majority pixel population had its values set to the median of the majority population. The resulting map was used to initialize a new run of the ICM algorithm. Validation was done by manually inspecting each field map and chemical decomposition for discontinuities and swapping errors. An error was significant only if it occurred inside of the main body of the animal.

Results

30% of the 134 images had significant swapping problems when extrapolation-initialization(5) wasn't used. With extrapolation-initialization, 8 images (6%) had significant errors. With the addition of error correction, 1 image (.7%) had significant errors. However, in three out of the 12 datasets, the automatically chosen starting slice did not yield good results, and a manually chosen slice had to be used. If only the results using the automatically chosen starting slice were considered, the error rate was 12% (16 images) without error correction. With error correction, the automatically chosen starting slice resulted in errors in 4 (3%) of the images. This represents a 88% improvement in error rate with the manually chosen starting slice, and a 75% improvement with the automatically chosen starting slice.

Discussion

We were able to use error correction to help compute globally smooth field maps and prevent partial swaps. However, the ability of the error correction to fix swaps depends on the ability of the algorithm to locate errors. Our combination approach allows for correction of most of the field map errors made by FLAWLESS because of the variety of errors it can detect. With extrapolation-initialization, complete swaps were avoided, which means that only partial swaps had to be detected. Without extrapolation-initialization, our error correction procedure was still able to correct partial swaps, but complete swaps remained a problem. Also, since we reinitialzed the error regions with the median of the entire non-error region, if the physical field inhomogeneity gradient is large, then this approach will result in swaps. Finally, if the source data contains artifacts like ghosting from motion, our algorithm, like other phase-based Dixon methods, will fail, since ghosting destroys the phase of the source data. Error correction requires additional computation time: the average was 130 seconds per image, about double that needed by FLAWLESS alone.

Conclusion

We have shown that error correction can be used to reliably and automatically decompose fat and water at 7T, with minimal human interference.

Acknowledgements

Thanks to Patiwet Wuttisarnwattana, Madhusudhana Gargesha, and Chris A. Flask. SN's effort was supported by F30DK082132 from NIDDK and T32GM07250 from NIGMS. The work was partly supported by an Ohio Biomedical Research and Technology Transfer award and C06 RR12463-01 from the NCRR. The content is solely the responsibility of the authors and does not necessarily represent the official views of the NIDDK, the NIGMS, NIBIB, the NCRR, or the NIH.

References

(1)Hines Radiology 2010 (2)Reeder JMRI 2009 (3)Reeder MRM 2005 (4)Lu MRM 2008 (5)Narayan JMRI 2011 (6)Hernando MRM 2008 (7)Dixon Radiology 1984

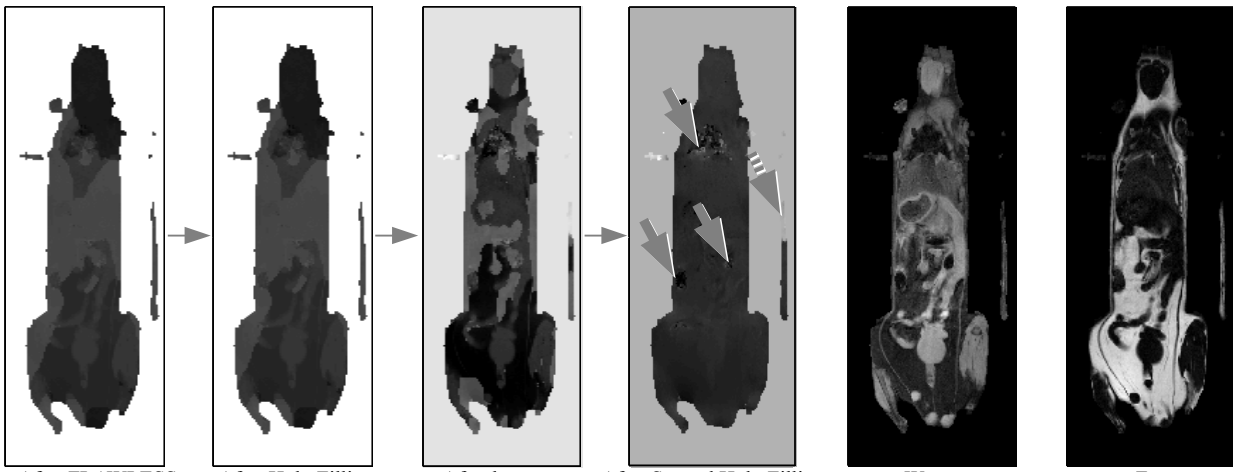

Figure 1: Results of Error Correction. In this example image, the swapping errors are corrected by our algorithms. Areas too small to be reached by the MRF regularization (dotted arrow) and spaces inside the animal (solid arrows) were not counted as significant errors. We have found the alternating pattern to be effective.